A Short-Term In Vivo Experimental Model for Fuchs Endothelial Corneal Dystrophy

M. Nour Haydari,[1,2] *Marie-Claude Perron,*[1] *Simon Laprise,*[3] *Olivier Roy,*[3] *J. Douglas Cameron,*[4] *Stéphanie Proulx,*[3] *and Isabelle Brunette*[1,2]

Purpose. We evaluated the in vivo functionality of a corneal endothelium tissue-engineered using corneal endothelial cells from human patients with Fuchs endothelial corneal dystrophy (FECD).

Methods. A total of 15 healthy cats underwent full-thickness corneal transplantation. All transplants were of xenogeneic human origin and all grafts but two were tissue-engineered. In seven animals the graft corneal endothelium was tissue-engineered using cultured corneal endothelial cells from humans with FECD (TE-FECD). Two control animals were grafted with an endothelium engineered using cultured endothelial cells from normal eye bank corneas (TE-normal). Two controls received a native full-thickness corneal transplant, and four other controls were grafted with the stromal carrier only (without endothelial cells). Outcome parameters included graft transparency (0, opaque to 4, clear), pachymetry, optical coherence tomography, endothelial cell morphometry, transmission electron microscopy (TEM), and immunostaining of function-related proteins.

Results. Seven days after transplantation, 6 of 7 TE-FECD grafts, all TE-normal grafts, and all normal native grafts were clear (transparency score >3), while all carriers-only grafts were opaque (score <1). The mean pachymetry was 772 ± 102 μm for TE-FECD, 524 ± 11 μm for TE-normal, 555 ± 48 for normal native, and 1188 ± 223 μm for carriers only. TEM showed subendothelial loose fibrillar material deposition in all TE-FECD grafts. The TE endothelium expressed Na^+-K^+/ATPase and Na^+/$HCO3^-$.

Conclusions. Restoration of transparency and corneal thickness demonstrated that the TE-FECD grafts were functional in vivo. This novel FECD seven-day living model suggests a potential role for tissue engineering leading to FECD cell rehabilitation. (*Invest Ophthalmol Vis Sci.* 2012;53:6343–6354) DOI: 10.1167/iovs.12-9708

Fuchs endothelial corneal dystrophy (FECD) is responsible for more than a quarter of the corneal transplantations performed in North America (28% of the 42,642 corneal grafts performed in the United States in 2010).[1] The pathophysiology of this inherited disease,[2–4] however, remains poorly understood. Corneal edema is thought to result from decreased endothelial cell density, increased endothelial permeability, and decreased endothelial pump function,[5–10] and there is mounting evidence that oxidative stress, DNA damage, and protein unfolding response leading to apoptosis may have a role in FECD pathogenesis.[11–16] Few experimental models are available to study FECD. A collagen VIII α2 Q455K knock-in mouse model recently has been developed successfully by Jun et al. for a rare type of early onset FECD.[17] He et al. cultured FECD corneal endothelial cells transfected with the human papillomavirus type 16 genes E6/E7 to expand their lifespan.[18] Culture of FECD cells has proved to be difficult without transfecting oncogenes.

Human corneal endothelial cells are arrested in the G1-phase of the cell cycle[19] and do not proliferate in vivo. However, they can proliferate in vitro in response to growth-promoting agents.[20–22] Our laboratory has shown that normal corneal endothelial cells can be cultured, and can retain function in vitro and in vivo.[23–25] We demonstrated to our knowledge the first evidence of successful culture, without viral transduction, of corneal endothelial cells from patients with FECD.[26] These cells also were used successfully to tissue engineer a corneal endothelium.[27]

In our study, we evaluated the functionality of a corneal endothelium tissue-engineered (TE) using corneal endothelial cells from human subjects with FECD, that were cultured on a devitalized human stromal carrier and transplanted in a living feline eye. This short-term in vivo experimental model for FECD was assessed and characterized.

Materials and Methods

All experiments were conducted in accordance with the Declaration of Helsinki and the ARVO Statement for the Use of Animals in Ophthalmic and Vision Research. The research protocol was approved by the Maisonneuve-Rosemont Hospital Animal Protection and Ethics for Clinical Research committees.

From the [1]Maisonneuve-Rosemont Hospital Research Center, Montreal, Québec, Canada; the [2]Department of Ophthalmology, University of Montreal, Montreal, Québec, Canada; the [3]Centre LOEX de l'Université Laval, Génie tissulaire et régénération - Centre de recherche FRSQ du Centre hospitalier affilié universitaire de Québec, Québec City, Québec, Canada, and Département d'ophtalmologie et d'oto-rhino-laryngologie, Faculté de médecine, Université Laval, Québec City, Québec, Canada; and the departments of [4]Ophthalmology and Laboratory Medicine and Pathology, Medical School, University of Minnesota, Minneapolis, Minnesota.

Supported by The Canadian Institutes for Health Research, Ottawa, ON, Canada (IB, SP), The FRQS Research in Vision Network, Montreal, QC, Canada (IB, SP), and by an unrestricted grant to the Department of Ophthalmology & Visual Neurosciences, University of Minnesota Medical School, Minneapolis, MN (JDC). IB is the recipient of the Charles-Albert Poissant Research Chair in Corneal Transplantation, University of Montreal, Canada.

Submitted for publication February 15, 2012; revised June 26, 2012; accepted August 15, 2012.

Disclosure: **M.N. Haydari**, None; **M.-C. Perron**, None; **S. Laprise**, None; **O. Roy**, None; **J.D. Cameron**, None; **S. Proulx**, None; **I. Brunette**, None

Corresponding author: Isabelle Brunette, Department of Ophthalmology, Maisonneuve-Rosemont Hospital, 5415 Boulevard de L'Assomption, Montreal, QC, H1T 2M4 Canada; i.brunett@videotron.ca.

Tissue Preparation

Consenting patients with FECD undergoing Descemet's stripping automated endothelial keratoplasty (DSAEK) or penetrating keratoplasty (PKP) for symptomatic nonreversible corneal endothelial failure at the Maisonneuve-Rosemont Hospital (Montreal) between October 2009 and September 2010 were enrolled in our study (four women and three men, aged 58–74 years, mean ± SEM 66 ± 6 years). At the time of DSAEK, the diseased Descemet's membrane (DM) and overlying endothelium were removed from the eye as described previously.[26] No viscoelastic agent was used. The specimen was put in Optisol-GS (Bausch and Lomb, Rochester, NY) and sent on ice to the laboratory for cell isolation. For PKP, the full thickness corneal specimen was sent in Optisol-GS and DM was stripped upon arrival in the laboratory.

FECD specimens were processed on the day following surgery. Endothelial cells were isolated as described by Zhu and Joyce.[22] In five cases, the cells were cryopreserved at P0 in 90% fetal bovine serum (Hyclone; Thermo Scientific, Waltham, MA)/10% dimethylsulfoxide (DMSO; Sigma, St. Louis, MO). The corneal endothelial cells were cultured as described previously[27] (Fig. 1A) and seeded at P1 ($n = 1$) or P2 ($n = 6$) (initial seeding of $2.42 \times 10^5 \pm 0.34 \times 10^5$ cells) on a devitalized human stroma, on which they were grown for 1 to 2 weeks (10.9 ± 1 days, range 8–15 days). The tissue-engineered corneas then were preserved in transport medium[25] for 1 to 3 days (2.5 ± 1 days, range 1–3) before transplantation.

A total of 13 eye bank corneas from 13 donors was used to produce stromal carriers (mean age ± SEM 62 ± 10 years, range 34–80 years). Native cells were killed through three freeze (−20°C)/thaw cycles and the devitalized corneas were stored at −20°C until used (mean delay of 70 ± 77 days, range 8–531 days). The carriers to be transplanted without endothelium were prepared in exactly the same manner, but without endothelial cell seeding.

For comparison purposes, two corneas also were engineered using the endothelial cells of normal eye bank corneas. The two donors were aged 68 and 47 years. Central Descemet's membrane was stripped using a circular biopsy punch (Acuderm; Dormer Laboratories, Toronto, ON, Canada) and fine forceps. Besides endothelial cell origin and isolation technique, all steps for tissue engineering of the normal and FECD corneas were identical.

Ultrastructure studies of mate nontransplanted, tissue-engineered corneas confirmed the previously reported similarity between the TE-FECD and TE-normal corneas in culture.[27] The endothelial monolayer was attached to DM, with well preserved nuclei, mitochondria, and rough endoplasmic reticulum (RER), all suggestive of healthy cellular activity (Fig. 1B). DM was normal, without guttae or subendothelial deposition of loose fibrillar material. The stroma was acellular.

For native controls, two normal eye bank corneas harvested within 12 hours after death were preserved in Optisol at 4°C and transplanted within 10 days after death. All eye bank tissues in our study were obtained from our local eye banks (Québec Eye Bank, Montréal, and Banque d'yeux du Centre universitaire d'ophtalmologie, Québec, QC, Canada) and were unsuitable for transplantation in humans.

Tissue Assignment

A total of 15 animals underwent full-thickness corneal transplantation. All transplants were of xenogeneic human origin and all grafts but two were tissue-engineered. Seven animals were grafted with a corneal endothelium tissue-engineered using endothelial cells from patients with FECD, cultured on a devitalized stromal carrier (TE-FECD grafts). Two control animals were grafted with a corneal endothelium tissue-engineered using endothelial cells from normal eye bank corneas, cultured on a devitalized stromal carrier (TE-normal grafts). Two control animals received a normal native human cornea (normal native grafts). Four other controls were grafted with the stromal carrier only, without endothelial cells (carrier-only). One eye per animal was assigned randomly to surgery, and the contralateral unoperated eye was used as a control.

Preoperative Management of the Animals

Healthy animals aged 8 to 27 months (mean ± SEM 13 ± 4 months) were obtained from a certified supplier. Standard ophthalmic examination of the animals included biomicroscopy (Haag-Streit, Bern, Switzerland), intraocular pressure measurement with a handheld veterinary tonometer (Tonovet, TV01; Tiolat Oy, Helsinki, Finland), and central corneal pachymetry (Ultrasound Pachymeter SP 3000; Tomey, Nagoya, Japan). Prophylactic famciclovir (Famvir; PMS, Montreal, QC) 125 mg/day per os was started on admission and continued over the entire study period.

Corneal Transplantation

Surgery was performed under general anesthesia, using the premedication, and systemic and topical medication described previously.[28] The donor cornea was warmed at room temperature over 2 hours before transplantation. It was cut with a 9-mm Hanna punch (Moria, Antony, France). The recipient cornea was cut with an 8-mm trephine Weck (Solan Medtronics, Jacksonville, FL) and the anterior chamber was filled with viscoelastic (Healon; AMO, Santa Ana, CA). The donor tissue was rinsed gently with balanced salt solution (BSS) and secured to the recipient bed with four cardinal sutures, followed by a 10–0 nylon single running suture (CU-1 10–0 nylon; Alcon Surgical, Fort Worth, TX). The viscoelastic was rinsed with BSS. A recombinant tissue plasminogen activator (150 μg in 0.3 mL; Alteplase, Genentech, CA) was injected into the anterior chamber to stimulate resorption of the gelatinous stands of fibrin, which tend to form in this species when the anterior chamber is entered. Suture knots were buried and the wound was checked for leaks using a fluorescein strip (fluorescein sodium ophthalmic strips; Chauvin Laboratories, Aubenas, France).

Postoperative Medication

At the end of surgery, all animals received subconjunctival injections of dexamethasone (1.2 mg in 0.3 mL), betamethasone (3 mg in 0.5 mL), tobramycin (10 mg in 0.25 mL), and cefazolin (55 mg in 0.25 mL), and an Elizabethan collar was installed. Sodium chloride 5% (Muro 128; Bausch & Lomb), tobramycin 0.3%, and dexamethasone 0.1% (Tobradex; Alcon) ointments were applied twice daily. Subconjunctival injections of dexamethasone (1.2 mg in 0.3 mL) or betamethasone (3 mg in 0.5 mL) were repeated when an increase in intraocular inflammation was observed on two consecutive days. No systemic antibiotics were given at any time.

Postoperative Follow-Up

Animals were examined daily by two independent observers. Graft transparency was quantified according to a subjective 0 to +4 scale, with +4 indicating a clear graft, +3 a slight opacity with iris/lens details easily visible, +2 mild opacity with iris/lens details still visible, +1 moderate opacity with no iris/lens details, and 0 an opaque cornea (iris not visible).[25] Anterior chamber cells and flare were quantified according to a 0 to +4 scale (for cells, in a field size of 1 × 1 mm slit beam, 0 indicated no cells, +1 indicated occasional cells, +2 indicated 8–15 cells, +3 too many to count, and +4 very dense. The flare scale was quantified as 0 empty, +1 very slight, +2 mild to moderate (iris/lens clear), +3 moderate (iris/lens hazy), and +4 severe (fibrin, plastic aqueous).[29] Intraocular pressure and central corneal thickness were measured on days 1, 2, 3, 4, and 7. When measurements exceeded the measuring limit of the pachymeter (1400 μm), this limit was used arbitrarily as the corneal thickness value.

Postmortem Assessment

Animals were euthanized (pentobarbital sodium 3 mL/2.5–5 kg intravenously) on postoperative day 7 (±12 hours) to avoid the acute immune reaction known to occur 9 to 14 days after transplantation.[30]

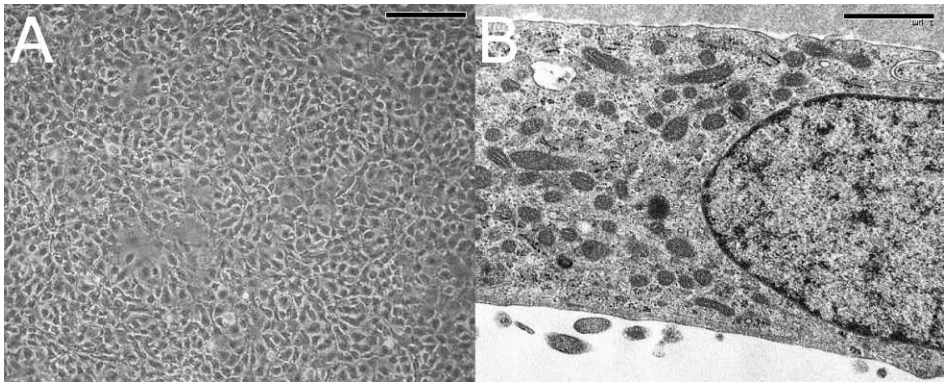

Figure 1. Corneal endothelial engineered using FECD endothelial cells. (**A**) FECD endothelial cells in culture. (**B**) TEM view of a mate nontransplanted cornea engineered by seeding FECD endothelial cells on a devitalized stromal carrier. The endothelial cell is attached to DM, and shows well preserved nucleus, numerous mitochondria and the presence of RER, all signs of healthy cellular activity. Note the absence of subendothelial deposition of loose fibrillar material. *Scale bars*: 200 μm (**A**) and 1 μm (**B**).

Operated and control eyes were enucleated and examined. Optical coherence tomography (OCT) was performed (OCT III or Visante 1000; Carl Zeiss Meditec, Dublin, CA) to assess graft thickness and to document the fine structures in the anterior chamber susceptible to be washed out during tissue processing for histology.

Corneal Endothelial Cell Density

Noncontact specular microscopy (Konan Medical INC., Nishinomiya, Hyogo, Japan) was performed on all eyes before surgery, while the postoperative cell counts were obtained from all eyes by vital staining of part of the excised corneas. The endothelium was stained with trypan blue (Sigma) and alizarin red S (Sigma),[31] and photographed (SteREO Discovery V12; Carl Zeiss Canada, Toronto, ON, Canada). Endothelial morphometric analyses were made using the KSS-409SP software (version 2.10; Cellchek XL; Konan Medical Inc., Irvine, CA). Three different fields were selected randomly for each corneal endothelium and a minimum of 100 cells per field were counted. The percentage of hexagonal cells was used as an index of pleomorphism and the coefficient of variation in cell area as a measure of polymegethism.[32,33]

Histopathology

A portion of each cornea was fixed in 10% neutral buffered formalin and paraffin embedded by standard techniques. Sections were cut at 5 μm, and stained with hematoxylin and eosin. A small portion of each cornea was fixed in 2.5% glutaraldehyde for transmission electron microscopy (H-7500; Hitachi, Tokyo, Japan).[23] For immunofluorescence staining, two samples of cornea were frozen in optimal cutting temperature solution (OCT; Somagen, Edmonton, AB, Canada). Indirect immunofluorescence assay was performed on acetone fixed cryosections, as described by Proulx et al.[25] Primary antibodies consisted of mouse monoclonal anti-Na+/K+-ATPase α1 (Millipore, Billerica, MA), and rabbit polyclonal anti–Na+/ HCO3 (Chemicon, Temecula, CA). After three rinses in PBS, sections were incubated for 30 minutes at room temperature with secondary antibodies consisting of goat anti–mouse IgG or chicken anti–rabbit antibodies conjugated with Alexa 594 (Invitrogen, Carlsbad, CA). Negligible background was observed for controls (primary antibodies omitted). Cell nuclei were counterstained with Hoechst reagent 33258.

Statistical Analyses

The Kruskal-Wallis exact test was used to test for differences in medians between groups. When the Kruskal-Wallis test was significant, pairwise comparisons were done with the exact Wilcoxon rank-sum test. The Pearson product-moment correlation coefficient was calculated when indicated. Mean values and SEM are reported, and a P value of less than 0.05 was considered to be statistically significant. All statistical tests were two-sided. The analyses were conducted using SAS 9.2 (SAS Institute, Rockville, MD).

Results

Surgery

Corneal transplantation was uncomplicated in all cases. In one of the carrier-only grafts, the running suture broke on the first day after surgery. It was re-sutured on the same day, but broke again on day 7. No reason could be identified for these repeated suture ruptures.

Post-Transplantation Follow-Up

Graft Transparency. TE-FECD grafts (Figs. 2A–D) and TE-normal grafts (Figs. 2E–H) were clear by biomicroscopy and OCT examination, although initially not as clear as the normal native grafts (Figs. 2I–L). The carrier-only controls remained opaque until the last day (Figs. 2M–P). Evolution of the mean graft transparency score as a function of time after transplantation is illustrated in Figure 3A. After seven days, the mean ± SEM score was 3.14 ± 0.76 (range 0.5–4) for the TE-FECD grafts, 3.25 ± 0.25 (range 3–3.5) for the TE-normal controls, 3.5 ± 0 for the normal native controls, and 0.56 ± 0.09 (range 0.5–0.75) for the carrier-only controls. The clinically significant difference in graft transparency observed between groups tended to be statistically significant (Kruskal-Wallis $P = 0.094$).

One of TE-FECD grafts behaved differently from the others. On the first day after surgery, a 360-degree posterior wound gap was noticed between the graft and recipient cornea, leading to recipient stromal edema at the wound. At day 4, the graft transparency score was 3 and the epithelium covered 60% of the graft surface. During the next following days, however, the epithelium was lost progressively and the exposed stroma rapidly became edematous, ulcerated, and necrotic, reducing the transparency score to 0.5 at day 7.

Pachymetry. The TE-normal grafts thinned continuously until their thickness reached that of the normal native controls (Fig. 3B). The TE-FECD grafts also thinned progressively, although not as completely as the TE-normal grafts. The normal native controls remained thin and the carriers-only remained thick throughout the entire study period. On postoperative day 7, the mean central thickness was 772 ± 102 μm (range 659–1023 μm) for the TE-FECD grafts, 524 ± 11

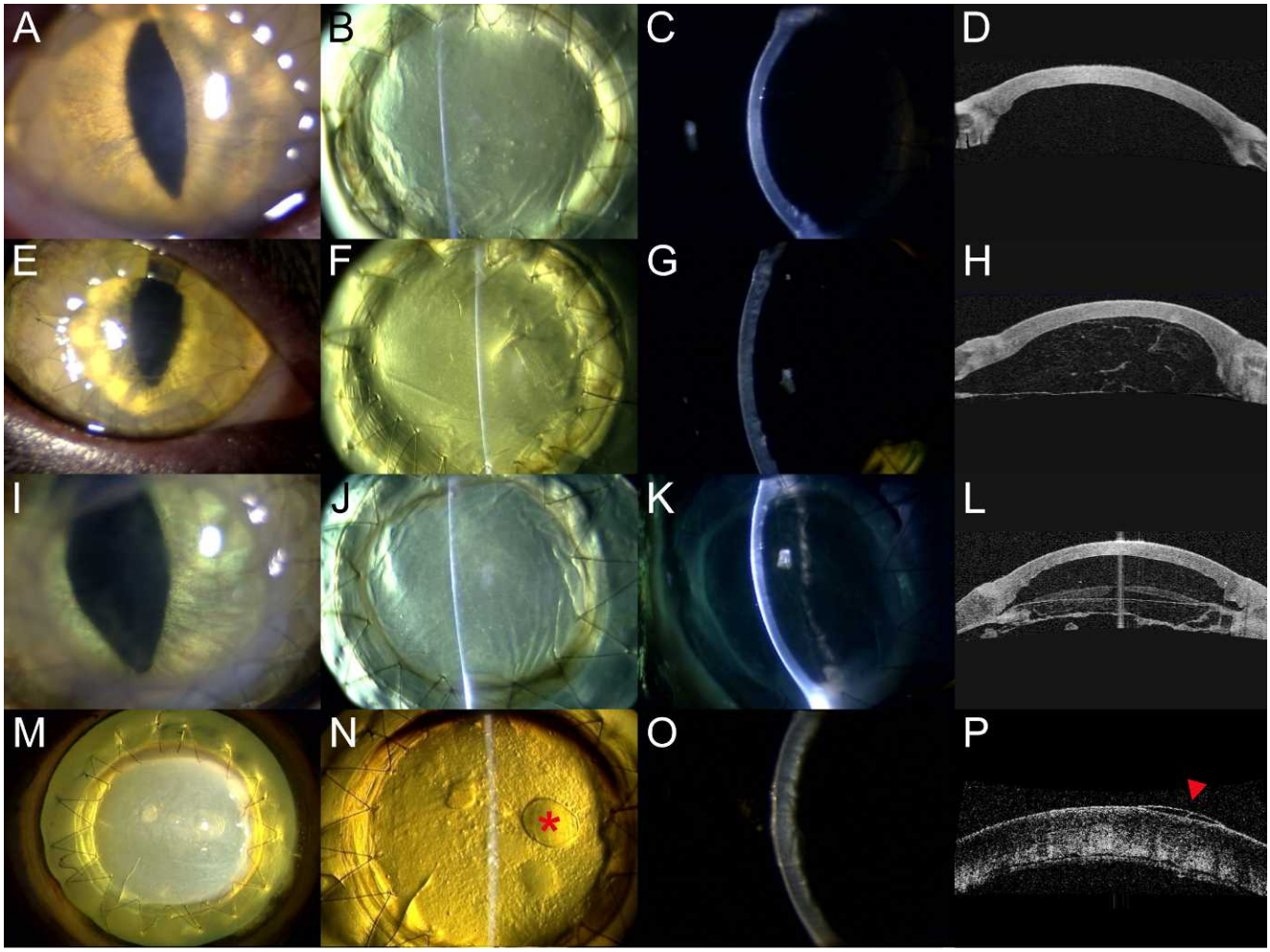

Figure 2. Corneal grafts 7 days after transplantation. Representative slit-lamp (*columns 1–3*) and OCT (*column 4*) photos are shown. (**A–D**) Tissue-engineered graft with endothelial cells from a patient with Fuchs dystrophy. The graft is clear and thin allowing visualization of fine iris structure. Our transparency score in this case was 3.75/4 and the central corneal thickness was 659 μm. (**E–H**) Corneal transplant tissue-engineered from normal human endothelial cells. The graft is clear and thin (transparency score 3.5/4, thickness 513 μm). A fine membrane of loose fibrin can be seen in the anterior chamber (**H**). (**I–L**) Normal native human corneal transplant. The graft is clear and thin (transparency score 3.5/4, thickness 507 μm). A fibrin membrane can be seen in the anterior chamber (**K–L**). (**M–P**) Tissue-engineered corneal transplant consisting of a devitalized carrier without endothelial cells. The graft is opaque and edematous, with large subepithelial bullae (*asterisk*, *arrow*) and no detailed view of the iris (transparency score 0.5/4, thickness 1400 μm).

(range 513–535 μm) for TE-normal controls, 555 ± 48 μm (range 507–603 μm) for normal native controls, and 1188 ± 223 μm (range 742–1400 μm) for carriers only. The Kruskal-Wallis test confirmed an overall significant difference in corneal thickness median values among the four groups at day 7 ($P = 0.0048$). Paired comparisons between TE-FECD and TE-normal grafts thicknesses tended to be statistically significant ($P = 0.07$), as did paired comparisons between TE-FECD and native grafts thicknesses ($P = 0.07$).

Reepithelialization. None of the tissue-engineered grafts was epithelialized at the time of transplantation. On day 7, six of the seven TE-FECD grafts were fully or almost fully re-epithelialized (mean coverage of 97.3 ± 3%, Fig. 3C). The case of corneal ulceration described above had practically no remaining epithelium at day 7. One of the two TE-normal grafts was fully re-epithelialized at day 7, while the epithelium of the other one remained fragile and edematous, covering only 25% of the graft surface at day 7. In one of the two normal native controls, the epithelium was removed during surgery, but grew back rapidly to achieve full coverage at day 7, and in the other case, the epithelium remained intact throughout the study period. The carrier-only controls were re-epithelialized at 97 ± 4% at day 7 in 3 out of 4 cases. In the fourth case, epithelial coverage reached 50% at day 4 and decreased to 20% at day 7.

Intraocular Pressure. Before surgery, the mean intraocular pressure for operated and nonoperated eyes was 31 ± 9 mm Hg. No significant increase in intraocular pressure was observed after surgery (Fig. 3D).

Intraocular Inflammation. All eyes were quiet before surgery. On the first postoperative day, mild intraocular inflammation was present in the anterior chamber of all eyes. The number of inflammatory cells decreased progressively during the following 3 to 4 days, with a tendency to increase again by the end of the week in all four groups (Fig. 3E). As the flare diminished (Fig. 3F), condensation of a fine fibrin formation reached its maximum at day 7. The fibrin deposition was characterized by spider-shaped filaments attaching to the edge of the graft and spreading over the graft posterior surface. The host cornea remained free of fibrin. Reactive inflammation is well known to be greater in the animal model than in human subjects.[34] Neovascularization was not present in any transplanted tissue.

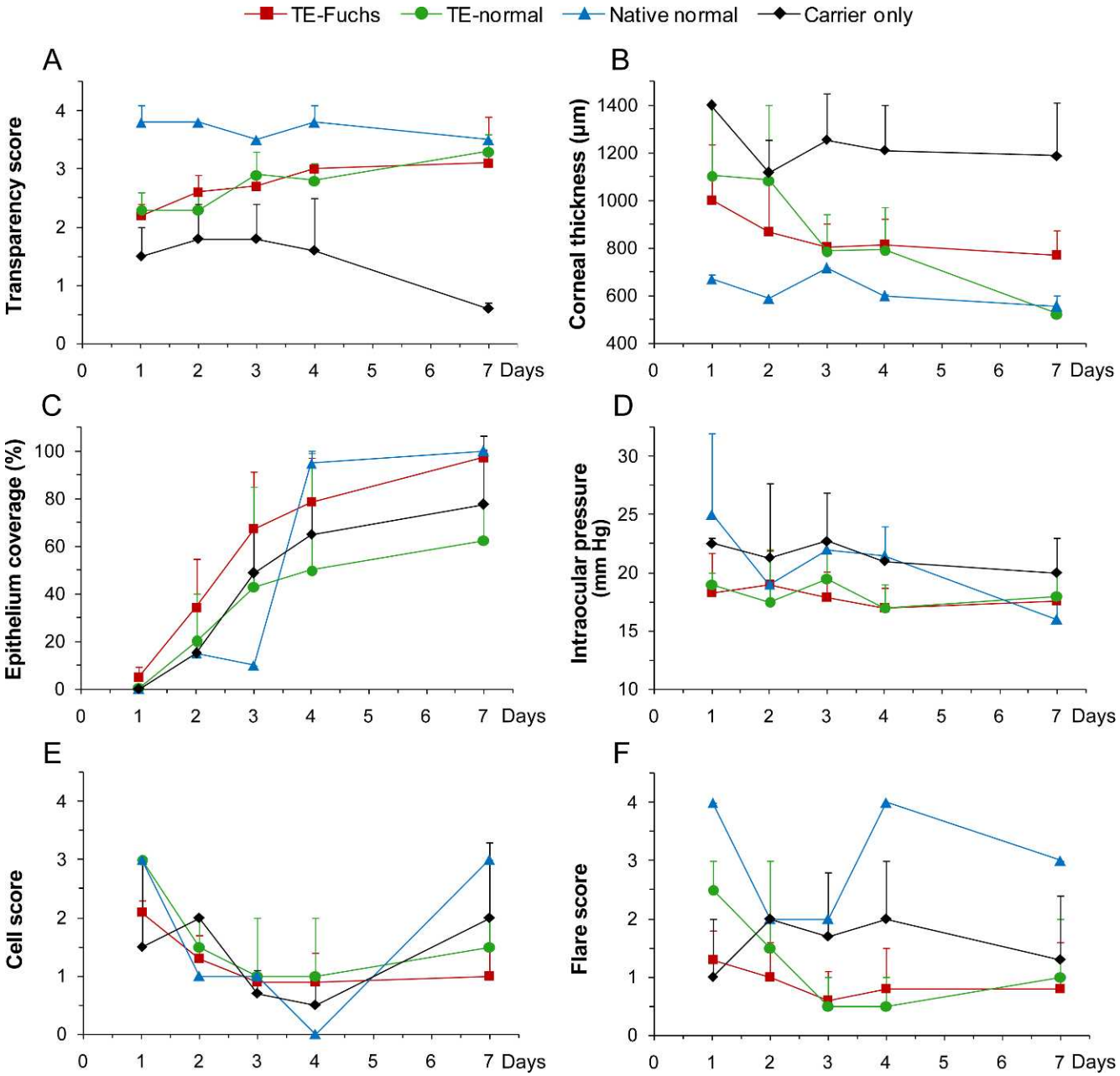

Figure 3. Clinical evolution of the operated eyes in the TE-FECD, TE-normal, normal native, and carrier-only groups. (**A**) Transparency score. (**B**) Corneal thickness. (**C**) Epithelial coverage. (**D**) Intraocular pressure. (**E**) Anterior chamber cell score. (**F**) Anterior chamber flare score. All study cases are represented in these graphs, except for epithelial coverage, cells and flare at day 7 for the TE-FECD complicated case with stromal ulceration. Mean values are reported and error bars represent SEM.

Endothelial Cell Counts and Morphometry

Tissue-engineered cells with an endothelial polygonal morphology in culture (as shown in Fig. 1A) maintained their morphology on the stromal carrier in culture and in vivo. Alizarin red and trypan blue vital staining 7 days after transplantation showed full coverage of DM by polygonal cells in the TE and native grafts (Fig. 4). Signs of endothelial stabilization and maturation of cell attachment were observed, with less space between cells than seen previously in culture. No endothelial cells were seen in any of the carrier-only controls ($n = 4$).

Seven days after transplantation, the average endothelial cell count was 966 ± 165 cells/mm^2 for TE-FECD grafts ($n = 5$), 1929 ± 200 cells/mm^2 for TE-normal controls ($n = 2$), and 2371 ± 44 cells/mm^2 for the normal native control ($n = 1$, see Table). Cell morphometric analyses could not be obtained in two TE-FECD grafts, that is in one case because of the presence of a fibrin membrane masking the endothelial cells, and in the other case because cells could not be seen due to stromal opacification (case of corneal necrosis described above). The Kruskal-Wallis test confirmed an overall significant difference in postoperative endothelial median cell counts among the three groups ($P = 0.036$). Interestingly, a strong negative correlation was observed between postoperative cell densities and central graft thickness at day 7 ($r = -0.914$, $P = 0.004$), all three groups being considered together.

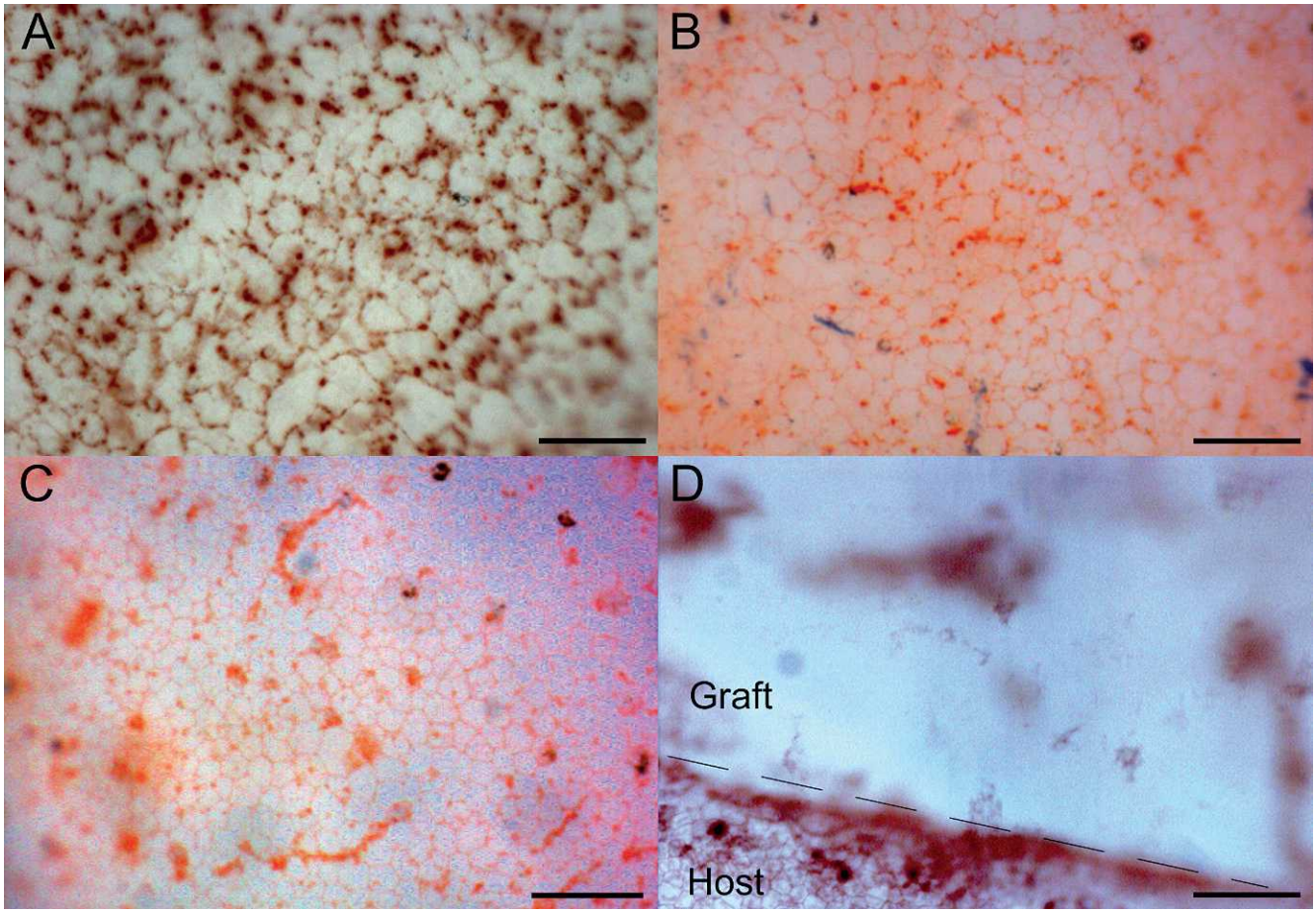

Figure 4. Alizarin red and trypan blue vital staining 7 days after transplantation. (**A**) TE-FECD living endothelial cells covering DM surface. The cells already have a polygonal contour. Some intercellular spaces can be seen (*dark spots*). Average ± SD cell count was 942 ± 445 cells/mm^2, average cell area was 1062 μm^2, CV was 42, 6-sided cells was 50%. (**B**) TE-normal endothelial cells seemed to be smaller with fewer intercellular spaces (average ± SD cell count was 1645 ± 336 cells/mm^2, average cell area was 608 μm^2, CV was 55, 6-sided cells was 55%). (**C**) Normal native endothelial cells were small, polygonal with no intercellular space (average ± SD cell count was 2198 ± 168 cells/mm^2, average cell area was 456 μm^2, CV was 37, 6-sided cells was 53%). (**D**) In the carrier-only controls, no endothelial cells were seen. *Scale bars*: 100 μm.

As a corollary, TE-FECD endothelial cells were larger than TE-normal and normal native controls. The Kruskal-Wallis test confirmed a significant difference in median cell area among the three groups at day 7 ($P = 0.036$). It also was interesting to notice that when the three groups were considered all together, cell area was correlated positively with graft thickness ($r = 0.785$, $P = 0.037$) and tended to be correlated negatively with graft transparency ($r = -0.685$, $P = 0.061$) at day 7.

Seven days after transplantation, the tissue-engineered endothelial cells reached a pattern closer to hexagonality than that observed in culture. Hexagonality is a sign of stability (contrary to endothelial mosaic disorganization, pleomorphism (differences in cell shape), and polymegethism (differences in cell sizes). In the TE-FECD group, 41 ± 5% of endothelial cells were hexagonal, compared to 41 ± 4% for the TE-normal and 51 ± 5% for the normal native grafts (see Table). The cell area coefficient of variation was 53 ± 10% for TE-FECD grafts, 51 ± 7% for TE-normal grafts, and 38 ± 3% for the normal native graft.

Histopathology

Light Microscopy. The corneal endothelial cells formed a monolayer in TE-FECD grafts in 6 cases (Fig. 5A). No guttae were seen in any case. The stroma was acellular, except in the periphery of the grafts where the keratocytes had started to migrate from the host stroma to the peripheral stroma of the graft. A small number of inflammatory cells were present in the stroma of three grafts. The restored epithelium consisted of 2 to 6 layers of cells that were well attached to graft Bowman's membrane in 6 cases. In the case with corneal ulceration, the anterior stroma of the graft was infiltrated massively with inflammatory cells, with foci of anterior corneal necrosis. No microorganisms were identified.

By light microscopy, TE-normal and TE-FECD grafts were very similar. In TE-normal grafts, the endothelial monolayer was well attached to DM (Fig. 5B), the host's keratocytes had started to migrate into the graft periphery, a few inflammatory cells were observed in the stroma of one of the grafts, and the regenerated epithelium consisted of 2 to 4 layers of cells well attached to Bowman's membrane.

The native controls showed a regular endothelial monolayer well attached to the underlying DM (Fig. 5C) and normal keratocytes present across the entire stroma. The epithelium consisted of 1 to 5 layers of cells well attached to Bowman's membrane.

In the carrier-only controls, no endothelial cells were seen. The otherwise acellular graft stroma had been repopulated partially by the host keratocytes in the periphery. Numerous inflammatory cells were observed within the stroma of two grafts and the epithelium consisted of only 1 to 3 layers of cells

Table. Endothelial Cell Counts and Morphology

	TE-FECD ($n = 5$)	TE-Normal ($n = 2$)	Normal Native ($n = 1$)	Carrier Only ($n = 4$)
Cell count, cells/mm^2	966 ± 165	1929 ± 200	2371 ± 44	0
Cell area, μm^2	1110 ± 248	528 ± 56	422 ± 8	N/A
SD of cell area	594 ± 157	268 ± 41	161 ± 13	N/A
CV of cell area	53 ± 10	51 ± 7	38 ± 3	N/A
6-sided cells, %	41 ± 5	41 ± 4	51 ± 5	N/A

Average ± SEM are reported. N/A, not applicable.

attached to Bowman's membrane. No neovascularization was seen in any of the 15 grafts.

Transmission Electron Microscopy (TEM). Overall, postmortem TEM confirmed the progression of tissue-engineered endothelial monolayer stabilization, with a maturation of the cell-cell attachments, fewer and narrower intercellular gaps, and more developed tight junctions than seen routinely in culture before transplantation.[27]

In the TE-FECD grafts, the endothelium consisted of a 1.5 to 2.5 μm thick monolayer of cells (Fig. 6A). Normal-appearing tight junctions were present (Fig. 6B). The endothelial cells generally were intact except that intercellular attachments were not always complete. Occasional apical V-shape separations of the cells (Fig. 6C) or a mid-height intercellular focal gaps (Fig. 6D) were present laterally. The endothelial nuclei were unremarkable (Figs. 6A, 6C, 6E). Numerous mitochondria were present (Fig. 6F). RER generally was prominent (Fig. 6G). Vacuoles were present in some cells, as well as electron dense bodies consistent with lysosomes (Fig. 6H). A focal zone of dense intracytoplasmic filaments was seen in one case (Fig. 6I). No pigment granules were present in any of the cases. Cytoplasmic processes were observed projecting either toward DM (Fig. 6J), toward the anterior chamber (microvilli, Fig. 6E), or toward a neighboring cell (Fig. 6D, arrows). The endothelium was attached to DM in all cases. Subendothelial deposition of loose fibrillar material was a consistent finding (Fig. 6K). The carrier's DM consisted of two normal anterior and posterior layers in all cases. No guttae were found in any of the cases. A few striated bodies (with a periodicity of 110 nm) were seen in the carrier's DM of one TE-FECD graft.

No apparently viable keratocytes were observed in TEM specimens, which is not surprising as TEM samples were cut from the center of the grafts. Nonviable keratocyte material was observed across the entire stroma (Fig. 6L), as remnants of the devitalization process. The space between stromal collagen fibers varied from 20 to 40 nm (Fig. 7A).

In the corneal ulceration case, the stroma was massively infiltrated with polymorphonuclear leukocytes and monocytes. Scattered degenerated endothelial cells were seen on the posterior surface of the graft.

In the TE-normal controls, the endothelium consisted of a 2.5 to 3.5 μm thick monolayer of cells (Fig. 8A). The attachment between adjacent endothelial cells generally was intact (Fig. 8B). Gaps between endothelial cells occasionally were seen and, when present, these gaps were less prominent than in the TE-FECD grafts. The endothelium was well attached to DM in all cases. Small amounts of subendothelial loose fibrillar material were observed in focal areas in one case. Small cytoplasmic processes were observed in one case projecting toward DM (Fig. 8C). Nuclei were intact. Vacuoles were seen, as well as electron dense bodies consistent with lysosomes. No pigment granules were seen. Mitochondria were unremarkable. RER was prominent (Fig. 8B). No intracellular filaments were seen. DM consisting of normal anterior and posterior layers was present in all the cases. No guttae were found. Residual nonviable keratocytes were observed in the stroma and the mean space between stromal collagen fibers was 25 nm (Fig. 7B).

In the normal native controls, the endothelium consisted of a 3.5-μm thick monolayer of cells (Fig. 8D). Adjacent endothelial cells were attached fully to each other and to underlying DM (Fig. 8E). Cell nuclei, mitochondria, and RER appeared normal (Fig. 8F). Vacuoles and lysosomes were observed. No cytoplasmic processes, pigment granules, intracellular filaments, or guttae were observed. DM consisted of normal anterior and posterior layers. Normal keratocytes were present throughout the stroma. The mean space between stromal collagen fibers was 15 nm (Fig. 7C).

TEM confirmed the absence of endothelial cells in the carrier-only controls. The DM was normal, without guttae. Residual nonviable keratocytes were observed in the stroma and the space between stromal collagen fibers was much larger, varying between 50 and 100 nm (Fig. 7D).

Immunofluorescence. Immunofluorescence detection of the sodium-potassium pump Na^+/K^+-ATPase α1 and the Na^+/HCO_3 cotransporter revealed the presence of these proteins in all three types of endothelialized grafts. However, staining was less intense in TE grafts than in the normal native grafts (Fig. 9).

Discussion

To the best of our knowledge, our study presents the first successful living model for FECD generated using untransformed human cells. We also demonstrated the first evidence that the sick endothelial cells of clinically decompensated FECD corneas, when cultured and seeded on a devitalized stromal carrier, can recover active pump function, and restore and maintain corneal transparency for 7 days after transplantation in the living feline eye.

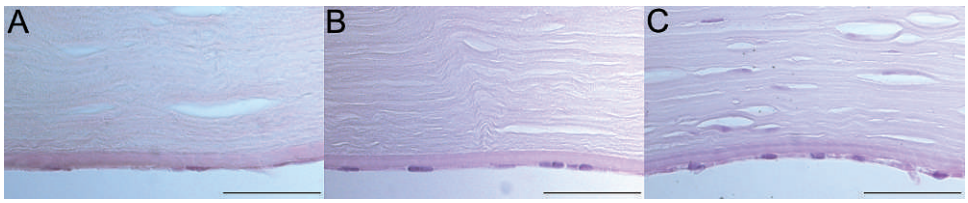

Figure 5. Histologic observations 7 days after transplantation. (**A**) TE-FECD graft. (**B**) TE-normal graft showing endothelium consisting of a continuous monolayer endothelial cells firmly adherent to DM. The stroma is acellular. (**C**) Normal endothelium of a native graft with native keratocytes in the stroma. Hematoxylin and eosin staining. *Scale bars*: 50 μm.

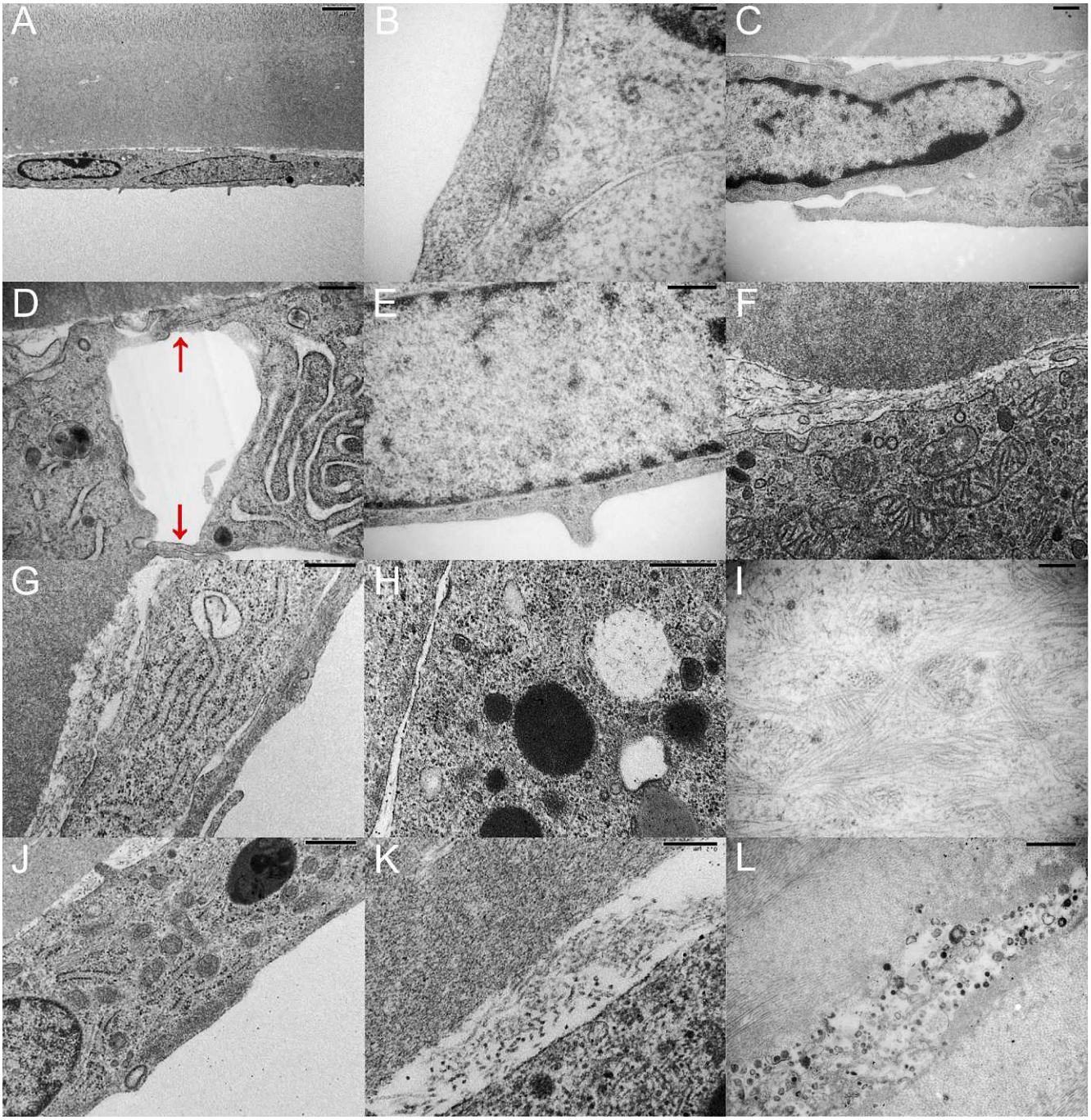

Figure 6. TEM. Ultrastructure of the TE-FECD grafts 7 days after transplantation. (**A**) Continuous monolayer of endothelial cells with intact nuclei. Normal DM. No guttata were present. (**B**) Complete cell-cell attachment showing tight junctions. (**C**) Incomplete apical cell-cell attachment. (**D**) Incomplete cell-cell attachment with intercellular residual gap. *Arrows*: indicate basal and apical cytoplasmic projections attaching two adjacent cells. (**E**) Microvillus oriented toward the anterior chamber. (**F**) Normal-appearing mitochondria. (**G**) Prominent RER with electron dense inclusion in Golgi apparatus. (**H**) Vacuoles and electron dense bodies consistent with lysosomes. (**I**) Intracytoplasmic filaments. (**J**) Cytoplasmic processes projecting toward DM. (**K**) Deposits of subendothelial fibrillar material. (**L**) Residual keratocyte debris in the devitalized stroma. *Scale bars*: 2 μm (**A**), 0.1 μm (**B**), 0.5 μm (**C–H, J**), 0.2 μm (**I, K**), and 1 μm (**L**).

Partial Rehabilitation

Overall, the tissue-engineered FECD endothelium seemed to perform better in the cat eye than in the patient's eye. TE-FECD grafts progressively became thinner and clearer. Rare trypan blue staining of the nuclei, TEM observation of a well structured TE-FECD endothelial monolayer, with developed tight junction complexes, normal mitochondria, enlarged RER (sign of active protein production), lysosomes, and vacuoles, as well as the presence of endothelial pump sites observed by immunofluorescence, all were signs of healthy cellular activity.

Explanations for this partial rehabilitation can be hypothesized only, since this was not investigated specifically in our study. Proposed hypotheses include the beneficial effect of the culture conditions and/or the natural selection of the healthiest cells in

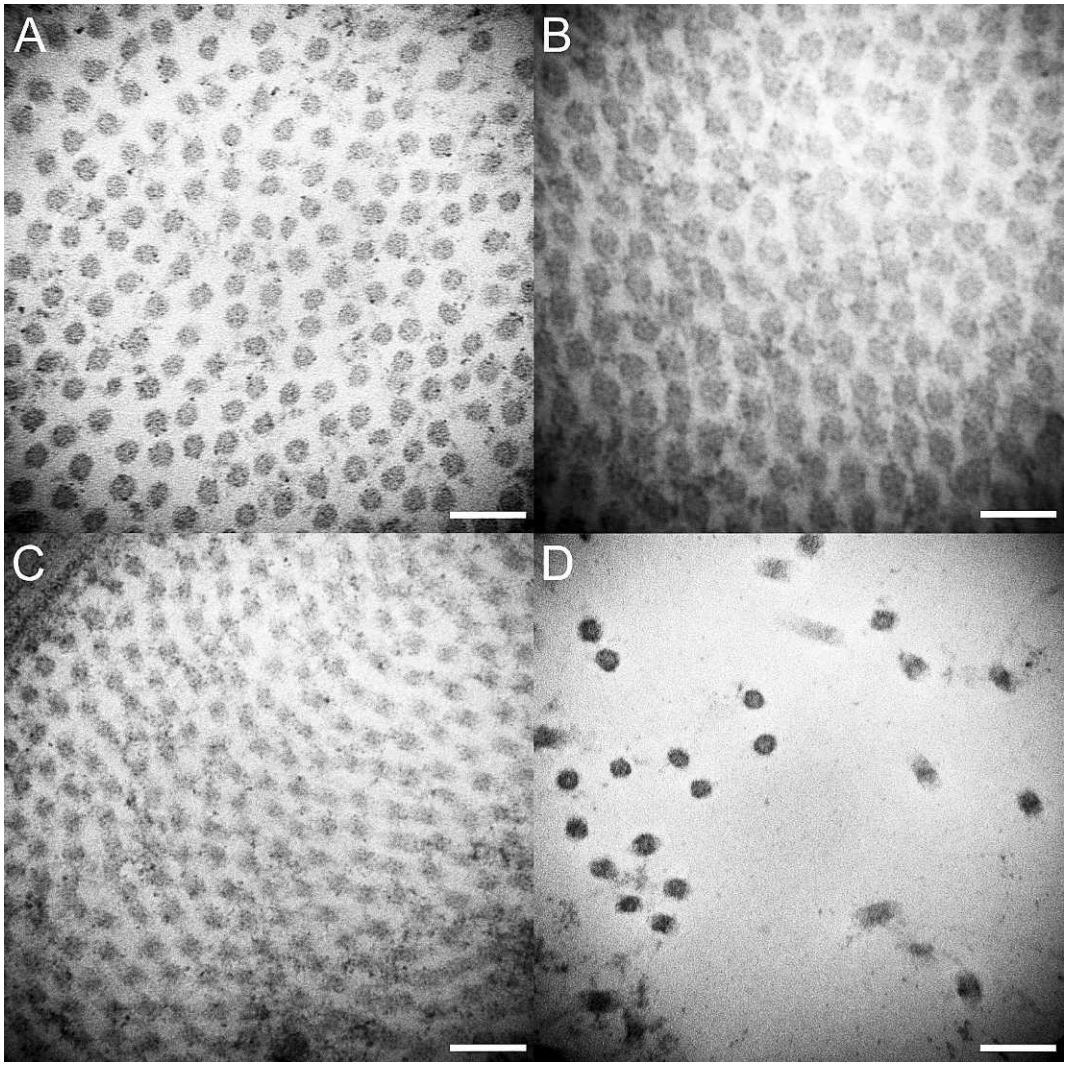

Figure 7. TEM. Stromal collagen fibers arrangement 7 days after transplantation. (**A**) TE-FECD graft showing a slightly irregular arrangement of the stromal collagen fibers. TE-normal graft (**B**) and normal native graft (**C**) showing a regular arrangement. (**D**) Carrier-only (without endothelial cells) grafts showing very irregular arrangement due to severe stromal edema. *Scale bars*: 100 nm.

culture. Removal of the diseased thickened DM also may have had a role in the recovery of these endothelial cells.

Partial rehabilitation of these end-stage FECD endothelial cells and the demonstration of their in vivo functionality opens the door to an entirely new horizon.

A Clinical Performance Suggestive of Early FECD

However, despite this functional improvement, the TE-FECD corneas still did not perform normally in vivo and these corneas rapidly had signs of mild-to-moderate Fuchs dystrophy. While considerably clearer and thinner than the negative controls without endothelium, the TE-FECD grafts remained thicker than the TE-normal and the native controls. Endothelial cell density also was lower in TE-FECD grafts.

TEM Signs Observed in Native and Tissue-Engineered FECD Corneas

Several of the TEM signs typically reported in native FECD corneas were observed in our study. Subendothelial deposition of a layer of loose fibrillar material was observed systematically in TE-FECD grafts. Some subendothelial amorphous or fibrillary material also was seen in one of the TE-normal grafts, but in focal areas only and in smaller amounts than in the TE-FECD grafts. This excessive basement membrane-like material production may reflect the known predisposition of FECD cells for excessive production of DM material. An abnormal thickening of DM is characteristic of native FECD, the normal anterior banded (fetal) and non-banded layers being lined typically by two abnormal layers consisting of a posterior banded layer and a fibrillar layer.[35–38]

Incomplete closure of the cell-cell attachments, fewer and shorter tight junctions, residual gaps between adjacent cells, and an overall lower cell density were observed in the TE-FECD grafts. This may suggest that FECD endothelial cells were more susceptible to death, the remaining cells spreading to reach the next available cell to cover the area left by dying cells. This process would be very similar to that described in native FECD, where degenerating endothelial cells loosen their junctional complexes and disintegrate, leaving large intercellular gaps.[36]

Intracytoplasmic filaments have been described by Iwamoto and DeVoe as a sign of transformation of the FECD endothelial cell into fibroblast-like cells,[36] but they also can be seen occasionally in the normal endothelium.[39] In our TEM

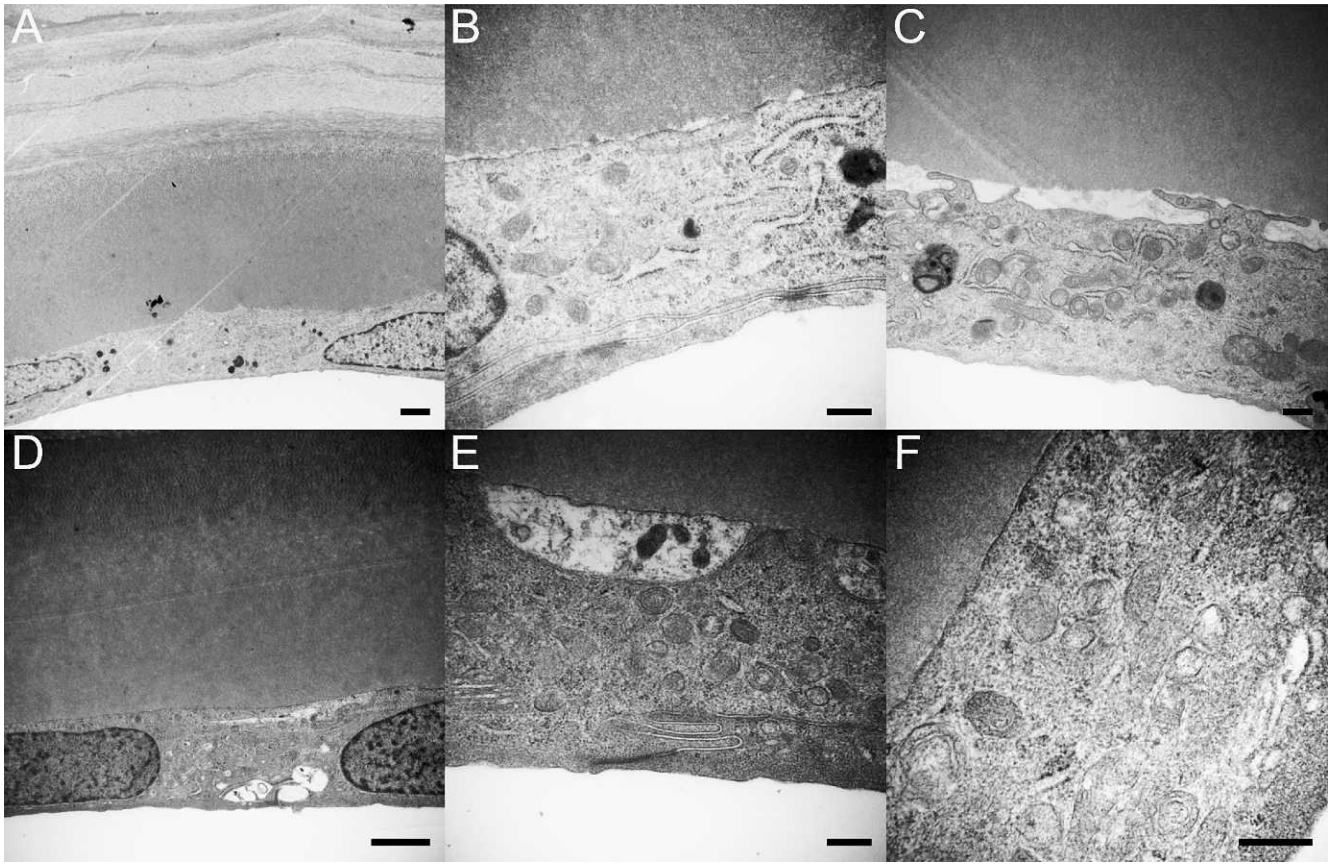

Figure 8. TEM. Ultrastructure of the TE-normal (**A–C**) and normal native (**D–F**) grafts 7 days after transplantation. (**A**) Continuous monolayer of endothelial cells with intact nuclei. (**B–C**) Complete cell-cell attachment with normal tight junctions. Prominent RER, normal-appearing mitochondria, electron dense bodies consistent with lysosomes, and cytoplasmic processes. Little subendothelial fibrillar material deposition. (**D**) Continuous monolayer of endothelial cells with normal nuclei. (**E**) Complete cell-cell attachment with mature tight junctions. Large vacuole-filled with cell debris. (**F**) Normal-appearing mitochondria and RER. Absence of cytoplasmic processes and subendothelial fibrillar material deposition. *Scale bars*: 2 μm (**A, D**) and 0.5 μm (**B–C, E–F**).

specimens, endothelial intracytoplasmic filaments were seen only once in a TE-FECD graft.

The pigment granules[36,40] seen in the patients' specimens were not recovered in any of the engineered endothelia. Pigment granules have been reported to originate from the iris pigmented epithelium and to be phagocytized normally by the corneal endothelial cells.[41] The absence of pigment in the tissue-engineered endothelium is not surprising in the absence of an active source (such as the iris pigmented epithelium). The pigment granules seen in the DSAEK specimens probably

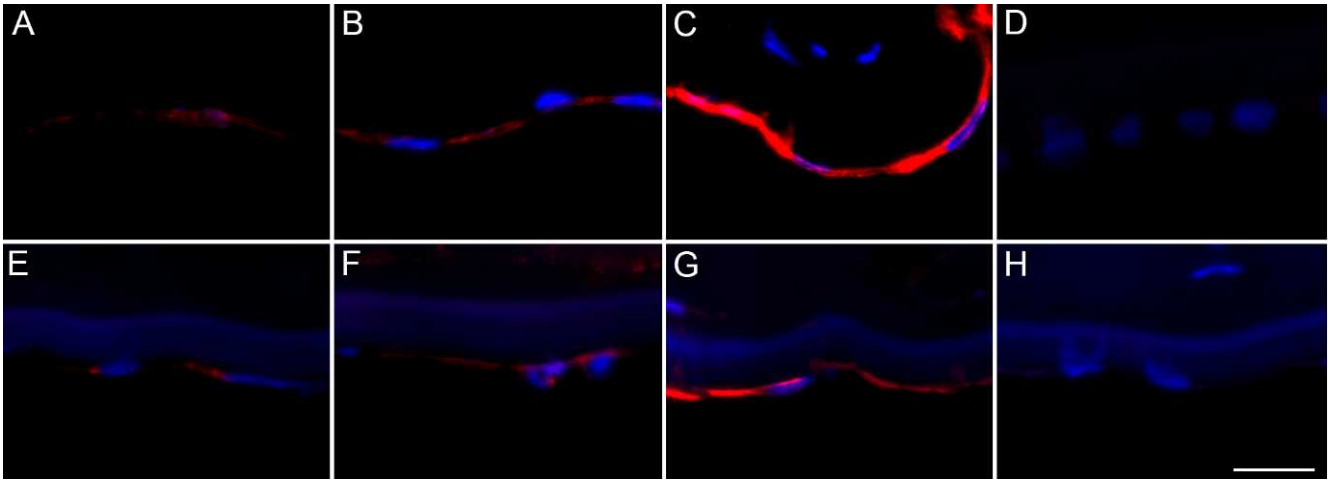

Figure 9. Immunofluorescence labeling of function-related proteins. Immunofluorescence detection of the sodium-potassium pump Na^+/K^+-ATPase α1 **(A–D)** and the Na^+/HCO_3 cotransporter **(E–H)** in a TE-FECD graft (**A, E**), a TE-normal graft (**B, F**), a normal native graft (**C, G**), and in negative controls (incubated with secondary antibody only, **D, H**). Cell nuclei were counterstained with Hoechst (*blue*). *Scale bar*: 20 μm.

were either rinsed off or eliminated with the loss of the most dysfunctional cells.

Striated bodies of various periodicity, size, and distribution are seen typically in the DM abnormal posterior banded layer and guttae of native corneas with FECD.[26,35,37,42,43] In our short-term study, no striated bodies were observed in the new DM-like material secreted by the engineered endothelium. No guttae formation were observed in our study, which also was compatible with the short duration of the follow-up.

In summary, in the absence of a single pathognomonic sign, the diagnosis of FECD usually is based on a combination of signs typical of the disease. In our study, all of the TE-FECD cells carried the genetic signature of the patient from whom they were harvested, and all these patients had a confirmed diagnosis of end-stage clinical FECD. Once transplanted back to a native living environment, this TE-FECD endothelium rapidly had a combination of signs typical of FECD, including low endothelial cell counts, corneal edema, incomplete cell-cell attachments, and the accelerated and excessive production of DM-like subendothelial material. After only 7 days in the living eye, this short-term model, which carries the genetic background of FECD, gathered the key descriptors for early FECD.

Characteristics of the Proposed FECD Model

The FECD model we describe offers several significant advantages. It is a living model, and it offers clinical and TEM quantifiable parameters for the characterization of TE-FECD endothelial function and structure. Clinical parameters include corneal transparency and corneal thickness (corneal transparency still is considered as the only real proof of endothelial functionality). TEM and histology parameters include a subendothelial layer of loose fibrillar material, which here appeared to be the most specific sign of FECD, and less specific signs, such as a decreased endothelial cell density, incomplete cell-cell attachment, and intracytoplasmic filaments. These parameters are very similar to those used to assess severity of the disease in native FECD**.** The model is polyvalent in that it is not limited to one specific mutation or cell line. In our study, no selection was made in the choice of FECD patients. The model allows for the in vivo selective investigation of FECD endothelial cell behavior in the absence of sick DM and guttae, and it allows for correlations between the FECD endothelial cells behavior in cell culture, in tissue culture, and in vivo, which can be very useful for the translational development of new therapies. Finally, it was developed in the feline eye, which is similar functionally to the human eye in several aspects. Feline corneal endothelial cells do not replicate in vivo,[44] contrary to species, such as the rat[45] or rabbit,[44,46] and the feline endothelium repairs by cell spreading and migration,[44] as in humans.[47] Endothelial cell density[48,49] and corneal thickness values are comparable to human values.[50,51] The large corneal diameter of the cat cornea (15.5–18 mm)[48,52] permits full size grafts, using the same instrumentation and techniques as for human subjects. These large grafts also yield large amounts of tissue for postmortem analyses. Finally, short term human-to-cat corneal xenografts are well tolerated.[53,54]

Additional improvements to this model could include a longer follow-up. A 7-day follow-up period was chosen here to avoid xenograft rejection. A longer follow-up would require immunosuppression.

Potential Applications of This Model

The living experimental model for FECD we describe suggested many novel research opportunities with a goal of better understanding of FECD cell dysfunction, molecular pathophysiology, and apoptosis. It offered the opportunity to test new therapeutic approaches at different stages of the disease.

In addition to the development of a new living model for FECD, our study confirmed the regenerative potential of FECD corneal endothelial cells in culture, making conceivable surgical therapeutic approaches in which the diseased corneal endothelial cells of Fuchs patients would be biopsied, cultured, treated, and used to engineer a healthy endothelium to be transplanted back to the patient (autograft). This would eliminate the risk of allograft rejection and constitute an exciting additional step toward a better management of this endothelial dystrophy.

In conclusion, we demonstrated to our knowledge the first evidence that the sick endothelial cells of clinically decompensated FECD corneas still retain proliferative capacity, allowing tissue engineering of a functional endothelium without transfection. Whether permitted by the favorable effect of the culture conditions or by the natural selection of the healthiest cells in culture, rehabilitation of end-stage FECD endothelial cells and the demonstration of their in vivo functionality opens the door to an entirely new horizon of medical and surgical therapies.

Acknowledgments

Patricia-Ann Laughrea obtained FECD endothelial specimens. Myriam Bareille, Danièle Caron, Patrick Carrier, André Deveault, Angèle Halley, Vivianne Leduc, Catherine Mauger Labelle, Aristide Pusterla, Olivier Rochette-Drouin, and the HMR-Rosemont and CUO operating room nurses provided technical assistance. Élodie Samson provided statistical analysis consultation. The LOEX research assistants provided the histology preparations. Fayrouz Barkat provided histology photography assistance, and Steve Breault provided the electron microscopy preparations and photography assistance.

References

1. *2010 Eye Banking Statistical Report*. Washington, DC: Eye Bank Association of America; 2011:18.
2. Rosenblum P, Stark WJ, Maumenee IH, Hirst LW, Maumenee AE. Hereditary Fuchs' dystrophy. *Am J Ophthalmol*. 1980;90:455–462.
3. Afshari NA, Li YJ, Pericak-Vance MA, Gregory S, Klintworth GK. Genome-wide linkage scan in Fuchs endothelial corneal dystrophy. *Invest Ophthalmol Vis Sci*. 2009;50:1093–1097.
4. Louttit MD, Kopplin LJ, Igo RP Jr, et al. A multicenter study to map genes for Fuchs endothelial corneal dystrophy: baseline characteristics and heritability. *Cornea*. 2012;31:26–35.
5. Burns RR, Bourne WM, Brubaker RF. Endothelial function in patients with cornea guttata. *Invest Ophthalmol Vis Sci*. 1981; 20:77–85.
6. Geroski DH, Matsuda M, Yee RW, Edelhauser HF. Pump function of the human corneal endothelium. Effects of age and cornea guttata. *Ophthalmology*. 1985;92:759–763.
7. Wilson SE, Bourne WM, O'Brien PC, Brubaker RF. Endothelial function and aqueous humor flow rate in patients with Fuchs' dystrophy. *Am J Ophthalmol*. 1988;106:270–278.
8. McCartney MD, Robertson DP, Wood TO, McLaughlin BJ. ATPase pump site density in human dysfunctional corneal endothelium. *Invest Ophthalmol Vis Sci*. 1987;28:1955–1962.
9. McCartney MD, Wood TO, McLaughlin BJ. Immunohistochemical localization of ATPase in human dysfunctional corneal endothelium. *Curr Eye Res*. 1987;6:1479–1486.
10. McCartney MD, Wood TO, McLaughlin BJ. Moderate Fuchs' endothelial dystrophy ATPase pump site density. *Invest Ophthalmol Vis Sci*. 1989;30:1560–1564.

11. Borderie VM, Baudrimont M, Vallee A, Ereau TL, Gray F, Laroche L. Corneal endothelial cell apoptosis in patients with Fuchs' dystrophy. *Invest Ophthalmol Vis Sci*. 2000;41:2501–2505.
12. Jurkunas UV, Bitar MS, Funaki T, Azizi B. Evidence of oxidative stress in the pathogenesis of Fuchs endothelial corneal dystrophy. *Am J Pathol*. 2010;177:2278–2289.
13. Jurkunas UV, Bitar MS, Rawe I, Harris DL, Colby K, Joyce NC. Increased clusterin expression in Fuchs' endothelial dystrophy. *Invest Ophthalmol Vis Sci*. 2008;49:2946–2955.
14. Jurkunas UV, Rawe I, Bitar MS, et al. Decreased expression of peroxiredoxins in Fuchs' endothelial dystrophy. *Invest Ophthalmol Vis Sci*. 2008;49:2956–2963.
15. Azizi B, Ziaei A, Fuchsluger T, Schmedt T, Chen Y, Jurkunas UV. p53-regulated increase in oxidative-stress-induced apoptosis in Fuchs endothelial corneal dystrophy: a native tissue model. *Invest Ophthalmol Vis Sci*. 2011;52:9291–9297.
16. Engler C, Kelliher C, Spitze AR, Speck CL, Eberhart CG, Jun AS. Unfolded protein response in fuchs endothelial corneal dystrophy: a unifying pathogenic pathway? *Am J Ophthalmol*. 2010;149:194–202.
17. Jun AS, Meng H, Ramanan N, et al. An alpha 2 collagen VIII transgenic knock-in mouse model of Fuchs endothelial corneal dystrophy shows early endothelial cell unfolded protein response and apoptosis. *Hum Mol Genet*. 2011;21:384–393.
18. He Y, Weng J, Li Q, Knauf HP, Wilson SE. Fuchs' corneal endothelial cells transduced with the human papilloma virus E6/E7 oncogenes. *Exp Eye Res*. 1997;65:135–142.
19. Joyce NC, Meklir B, Joyce SJ, Zieske JD. Cell cycle protein expression and proliferative status in human corneal cells. *Invest Ophthalmol Vis Sci*. 1996;37:645–655.
20. Joyce NC. Proliferative capacity of the corneal endothelium. *Prog Retin Eye Res*. 2003;22:359–389.
21. Joyce NC, Zhu CC. Human corneal endothelial cell proliferation: potential for use in regenerative medicine. *Cornea*. 2004; 23:S8–S19.
22. Zhu C, Joyce NC. Proliferative response of corneal endothelial cells from young and older donors. *Invest Ophthalmol Vis Sci*. 2004;45:1743–1751.
23. Proulx S, Audet C, Uwamaliya J, et al. Tissue engineering of feline corneal endothelium using a devitalized human cornea as carrier. *Tissue Eng Part A*. 2009;15:1709–1718.
24. Proulx S, d'Arc Uwamaliya J, Carrier P, et al. Reconstruction of a human cornea by the self-assembly approach of tissue engineering using the three native cell types. *Mol Vis*. 2010; 16:2192–2201.
25. Proulx S, Bensaoula T, Nada O, et al. Transplantation of a tissue-engineered corneal endothelium reconstructed on a devitalized carrier in the feline model. *Invest Ophthalmol Vis Sci*. 2009;50: 2686–2694.
26. Zaniolo K, Bostan C, Rochette Drouin O, et al. Culture of human corneal endothelial cells isolated from corneas with Fuchs endothelial corneal dystrophy. *Exp Eye Res*. 2012;94:22–31.
27. Goyer B, Haydari MN, Drouin OR, et al. Tissue engineering of a corneal endothelium using cells from patients with Fuchs endothelial corneal dystrophy. Tissue Eng. In press.
28. Brunette I, Rosolen SG, Carrier M, et al. Comparison of the pig and feline models for full thickness corneal transplantation. *Vet Ophthalmol*. 2011;14:365–377.
29. Schlaegel TJ. *Essentials of Uveitis*. Boston: Little, Brown & Co; 1969.
30. Bahn CF, MacCallum DK, Lillie JH, Meyer RF, Martonyi CL. Complications associated with bovine corneal endothelial cell-lined homografts in the cat. *Invest Ophthalmol Vis Sci*. 1982; 22:73–90.
31. Taylor MJ, Hunt CJ. Dual staining of corneal endothelium with trypan blue and alizarin red S: importance of pH for the dye-lake reaction. *Br J Ophthalmol*. 1981;65:815–819.
32. Matsuda M, Bourne WM. Long-term morphologic changes in the endothelium of transplanted corneas. *Arch Ophthalmol*. 1985; 103:1343–1346.
33. McCarey BE, Edelhauser HF, Lynn MJ. Review of corneal endothelial specular microscopy for FDA clinical trials of refractive procedures, surgical devices, and new intraocular drugs and solutions. *Cornea*. 2008;27:1–16.
34. Short BG. Safety evaluation of ocular drug delivery formulations: techniques and practical considerations. *Toxicol Pathol*. 2008; 36:49–62.
35. Yuen HK, Rassier CE, Jardeleza MS, et al. A morphologic study of Fuchs dystrophy and bullous keratopathy. *Cornea*. 2005;24: 319–327.
36. Iwamoto T, DeVoe AG. Electron microscopic studies on Fuchs' combined dystrophy. I. Posterior portion of the cornea. *Invest Ophthalmol*. 1971;10:9–28.
37. Bourne WM, Johnson DH, Campbell RJ. The ultrastructure of Descemet's membrane. III. Fuchs' dystrophy. *Arch Ophthalmol*. 1982;100:1952–1955.
38. Waring GO 3rd. Posterior collagenous layer of the cornea. Ultrastructural classification of abnormal collagenous tissue posterior to Descemet's membrane in 30 cases. *Arch Ophthalmol*. 1982;100:122–134.
39. Iwamoto T, Smelser GK. Electron microscopy of the human corneal endothelium with reference to transport mechanisms. *Invest Ophthalmol*. 1965;4:270–284.
40. Bergmanson JP, Sheldon TM, Goosey JD. Fuchs' endothelial dystrophy: a fresh look at an aging disease. *Ophthalmic Physiol Opt*. 1999;19:210–222.
41. Bloomfield SE, Jakobiec FA, Iwamoto T, Harrison WG. Retrocorneal pigmentation secondary to iris stromal melanocytic proliferation. *Ophthalmology*. 1981;88:1274–1280.
42. Gottsch JD, Zhang C, Sundin OH, Bell WR, Stark WJ, Green WR. Fuchs corneal dystrophy: aberrant collagen distribution in an L450W mutant of the COL8A2 gene. *Invest Ophthalmol Vis Sci*. 2005;46:4504–4511.
43. Kayes J, Holmberg A. The fine structure of the cornea in Fuchs' endothelial dystrophy. *Invest Ophthalmol*. 1964;3:47–67.
44. Van Horn DL, Sendele DD, Seideman S, Buco PJ. Regenerative capacity of the corneal endothelium in rabbit and cat. *Invest Ophthalmol Vis Sci*. 1977;16:597–613.
45. Tuft SJ, Williams KA, Coster DJ. Endothelial repair in the rat cornea. *Invest Ophthalmol Vis Sci*. 1986;27:1199–1204.
46. Nakahori Y, Katakami C, Yamamoto M. Corneal endothelial cell proliferation and migration after penetrating keratoplasty in rabbits. *Jpn J Ophthalmol*. 1996;40:271–278.
47. Joyce NC, Meklir B, Neufeld AH. In vitro pharmacologic separation of corneal endothelial migration and spreading responses. *Invest Ophthalmol Vis Sci*. 1990;31:1816–1826.
48. Bahn CF, Glassman RM, MacCallum DK, et al. Postnatal development of corneal endothelium. *Invest Ophthalmol Vis Sci*. 1986;27:44–51.
49. Giasson CJ, Gosselin L, Masella A, Forcier P. Does endothelial cell density correlate with corneal diameter in a group of young adults? *Cornea*. 2008;27:640–643.
50. Gonzalez-Perez J, Gonzalez-Meijome JM, Rodriguez Ares MT, Parafita MA. Central corneal thickness measured with three optical devices and ultrasound pachometry. *Eye Contact Lens*. 2011;37:66–70.
51. Bourne WM, Nelson LR, Buller CR, Huang PT, Geroski DH, Edelhauser HF. Long-term observation of morphologic and functional features of cat corneal endothelium after wounding. *Invest Ophthalmol Vis Sci*. 1994;35:891–899.
52. Carrington SD, Woodward EG. Corneal thickness and diameter in the domestic cat. *Ophthalmic Physiol Opt*. 1986;6:385–389.
53. Ohno K, Nelson LR, Mitooka K, Bourne WM. Transplantation of cryopreserved human corneas in a xenograft model. *Cryobiology*. 2002;44:142–149.
54. Bahn CF, Meyer RF, MacCallum DK, et al. Penetrating keratoplasty in the cat. A clinically applicable model. *Ophthalmology*. 1982;89:687–699.